

High-Temperature Stability of the Phase Composition of Langasite Family Crystals

O. M. Kugaenko^a, S. S. Bazalevskaya^{a,c}, T. B. Sagalova^a, V. S. Petrakov^b,
O. A. Buzanov^c, and S. A. Saharov^c

^aNational University of Science and Technology (MISIS), Moscow, 119049 Russia

^bInstitute of Economics and Power Engineering, Moscow, 111250 Russia

^cOAO Fomos-Materials, Moscow, 107023 Moscow

e-mail: crystalxxi@mis.ru

Abstract—Thermal stability of the phase composition of langasite family crystals is studied by means of high-temperature X-ray diffractometry upon heating in vacuo and in air. Upon heating above 1000°C in vacuo, the partial decomposition of the initial phase is observed in $\text{La}_3\text{Ga}_5\text{SiO}_{14}$, $\text{La}_3\text{Ta}_{0.5}\text{Ga}_{5.5}\text{O}_{14}$, and $\text{Ca}_3\text{TaGa}_3\text{Si}_2\text{O}_{14}$ crystals; this is accompanied by the emergence of gallium-depleted oxides of the main elements, due to the formation of volatile gallium protoxide and the loss of gallium in the surface layer of the crystals. Langasite family crystals are found to be stable when annealed in air up to a temperature of 1200°C.

DOI: 10.3103/S106287381410013X

INTRODUCTION

Lanthanum–gallium silicate family crystals are new domestically produced compounds whose properties are superior to those of the main material of piezoelectric technology, stable and high-Q crystallize quartz. Their advantages include a high electromechanical coupling factor (three times that of quartz) and a lack of phase transitions, making the langasite family of crystals piezoactive up to their melting point. Langasite crystals were discovered in the 1980s by B.V. Mill, M.F. Dubovik, G.D. Mansfeld, I.M. Silvestrova, and Yu.V. Pisarevsky [1, 2]. More than one hundred compounds of this family are known today, and OAO Fomos-Materials is active in the synthesis and treatment of lanthanum–gallium silicate family crystals [3, 4].

The use of langasite-based piezoelectric elements in acoustoelectronics is now widespread [5, 6]. The crystals are used at temperatures ranging from room to 600°C as thermostable wideband monolithic filters in mobile telephony; piezoelectric elements in sensors of pressure, vibration, and detonation; and substrates for thermostable slices in acoustoelectric filters of surface and bulk acoustic waves. The crystals must maintain their operating capabilities at the high temperatures and thermomechanical loads of internal combustion engines, nuclear reactors, rotors of aircraft engines, and space exploration. Studies of the thermal stability of the structure and properties of the crystals are needed to expand the operating temperature interval in which they can be used in modern high-temperature sensor acoustic and piezoelectric technology.

The aim of this work was to study the thermal stability of the phase composition of lanthanum–gallium silicate family crystals (langasite ($\text{La}_3\text{Ga}_5\text{SiO}_{14}$), langatate ($\text{La}_3\text{Ta}_{0.5}\text{Ga}_{5.5}\text{O}_{14}$), and catangasite ($\text{Ca}_3\text{TaGa}_3\text{Si}_2\text{O}_{14}$)) upon annealing in vacuo and in air in the temperature range of 25 to 1200°C by means of high-temperature X-ray diffractometry.

EXPERIMENTAL

Our materials of study were single langasite family crystals grown using the Czochralski method at OAO Fomos-Materials. Langasite family crystals are isostructural with calcium–gallium germanate ($\text{Ca}_3\text{Ga}_2\text{GeO}_{14}$) of trigonal syngony, symmetry class 32, and space group $P321$. A layered structure forms during crystal growth that consists of coordination polyhedra (Fig. 1) [1, 2]. Layers with tetrahedral positions and layers with octahedral and dodecahedral positions alternate along the Z axis. Comparing langasite family crystals to structures of $\text{Ca}_3\text{Ga}_2\text{GeO}_{14}$, we notice that lanthanum La^{3+} occupies the dodecahedral positions of Ca, while gallium Ga^{3+} occupies the tetrahedral and octahedral positions of Ga and Ge. Depending on which ion is substituted for gallium in the corresponding position, the material is either langasite (with Si^{3+} in the tetrahedral position) or langatate (with Ta^{5+}) [1, 2].

The position of cation A in the center of a Thomson cube made of eight oxygen atoms (AO_8) is occupied by such large cations as Ca^{2+} or La^{3+} . Cations with oxidation levels of 2+ to 6+ occupy octahedral position B (BO_6). Positions C and D are surrounded by oxygen tetrahedra CO_4 and DO_4 . Cations with longer radii occupy position C ; those with shorter radii, position D .

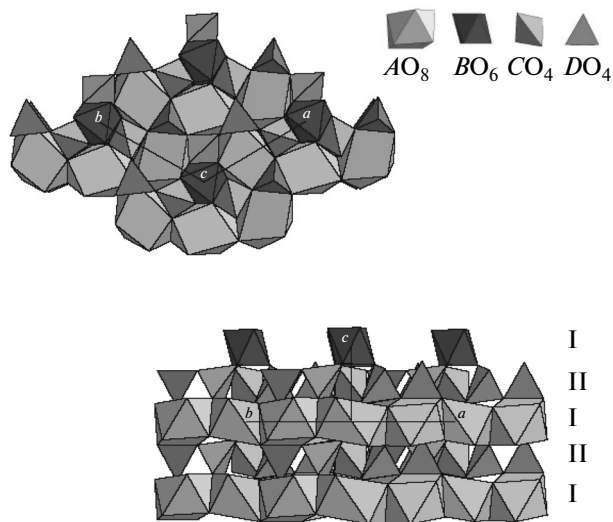


Fig. 1. Structural model of calcium-gallium germanate ($A_3BC_3D_2O_{14}$) [1]. Upper part: projection [0001]; bottom part: projection $[\bar{1}\bar{1}20]$.

Numerous compounds of the lanthanum–gallium silicate crystal family are possible due to the substitution of cations.

The structure of lanthanum–gallium tantalate LGT ($La_3Ga_{5.5}Ta_{0.5}O_{14}$) contains layers of $(Ga,Ta)O_4$ tetrahedra that are in turn connected through Ga^{3+} ions in the octahedral positions and La^{3+} ions in an octuple positions (twisted Thomson cubes). The tetrahedral Ga^{3+} ions are statistically distributed over the corresponding positions in a structure with Ta^{5+} ions.

Imperfections are found in the structure of langasite family crystals because cations of two types occupy the same position of a crystal unit in each compound (langasite and langatate). These are Ga^{3+} and Si^{4+} in langasite and Ga^{3+} and Ta^{5+} in langatate. This results in stochastically distributed distortions in the structure and thus changes in its properties. For instance, the piezoelectric coefficients and size of a crystal unit increase when the Si^{4+} ion ($r_{Si} = 0.26 \text{ \AA}$) in the trigonal pyramid is replaced with Ga^{4+} ($r_{Ga} = 0.47 \text{ \AA}$).

The structure of langasite crystals has different lattice parameters along the Z and X directions (Table 1)

[2], which is typical of crystals with trigonal syngony and prominent anisotropy.

High-temperature X-ray diffraction studies of the thermal stability of the phase composition were conducted using powder samples of $La_3Ga_5SiO_{14}$, $La_3Ta_{0.5}Ga_{5.5}O_{14}$, and $Ca_3TaGa_3Si_2O_{14}$ (ground monocrystals) placed in a special container; the maximum size of the powder particles did not exceed $200 \mu\text{m}$.

Measurements were performed on a Bruker D8 Advance X-ray diffractometer via symmetrical θ – 2θ scanning with monochromatic $CuK\alpha$ radiation ($\lambda = 1.54178 \text{ \AA}$). The vacuum was kept at 10^{-3} Torr. The samples were heated from 25 to 1200°C in steps of 100 – 200°C at a heating rate of 0.5°C s^{-1} with isothermal exposure for 1 h after every 200°C step. Each isothermal exposure was followed by the acquisition of the X-ray diffraction pattern over 0.5 h in the range of $\theta/2\theta = 10^\circ$ – 70° with angle steps of 0.1° and pulse accumulation durations of 3 s. The powder was thus annealed over 1.5 h in steps of 100 – 200°C (500 , 600 , 900 , 1000 , 1100 , and 1200°C) during our measurements.

To analyze the changes in the intensities and angular positions of individual peaks, diffraction patterns were measured repeatedly with the same temperature intervals and exposures. To investigate the aging of langatate over longer periods of annealing, a series of measurements was performed at 600 and 1000°C and exposure times of 6 h in vacuo, and after isothermal annealing at 1200°C in the same regime in air.

Diffraction reflections were identified by using the EVA software to compare the experimental values of interplanar spacings and the standard values for various compounds listed in the powder diffractometry database ICDD PDF-2 (2006).

The depth of X-ray penetration into the studied crystals was calculated to estimate the depth of the surface layers, which were analyzed via X-ray phase analysis. Intensity $I(x)$ of the electromagnetic radiation propagating in a solid medium diminishes with depth x according to the Beer–Lamber–Bouguer law (1):

$$I(x) = I(0)\exp(-\mu x), \quad (1)$$

where $I(0)$ is the intensity of the incident radiation, $I(x)$ is the intensity at depth x ; and μ is the linear attenuation coefficient, cm^{-1} .

Table 1. Crystallographic characteristics of langasite, langatate, catangasite, and quartz

Compounds	Langasite ($La_3Ga_5SiO_{14}$)	Langatate ($La_3Ga_{5.5}Ta_{0.5}O_{14}$)	Catangasite ($Ca_3TaGa_3Si_2O_{14}$) [7]	Quartz
Lattice parameters, 10^{-10}m	$a_0 = 8.162$ $c_0 = 5.087$ $c_0/a_0 = 0.6233$	$a_0 = 8.228$ $c_0 = 5.124$ $c_0/a_0 = 0.6228$	$a_0 = 8.09831$ $c_0 = 4.97694$ $c_0/a_0 = 0.6146$	$a_0 = 4.9133$ $c_0 = 5.4053$ $c_0/a_0 = 0.9090$
Unit cell volume, 10^{-30} m^3	0.293	0.300	0.282	0.113

Table 2. Phase composition of the investigated powders: high-temperature measurements *in vacuo* and after annealing in air

Item no.	Crystal	Measuring temperature, °C	Phase composition	
			main	additional
1	Langasite	400–1000	La ₃ Ga ₅ SiO ₁₄	None
		1200 (vacuum)	La ₃ Ga ₅ SiO ₁₄	La(GaO ₃) La ₂ O ₃
		1200 (air)	La ₃ Ga ₅ SiO ₁₄	None
2	Langatate	400–1000	La ₃ Ta _{0.5} Ga _{5.5} O ₁₄	None La(TaO ₄) La(GaO ₃) TaO ₂
		1200 (vacuum)	La ₃ Ta _{0.5} Ga _{5.5} O ₁₄	None
		1200 (air)	La ₃ Ta _{0.5} Ga _{5.5} O ₁₄	None
3	Catangasite	400–1000	Ca ₃ TaGa ₃ Si ₂ O ₁₄	None CaSiO ₃ Ca ₂ Ta ₂ O ₇
		1200 (vacuum)	Ca ₃ TaGa ₃ Si ₂ O ₁₄	None
		1200 (air)	Ca ₃ TaGa ₃ Si ₂ O ₁	None

For X-ray radiation with wavelength $\lambda_{\text{CuK}\alpha} = 1.54 \times 10^{-10}$ m, the maximum depth of an analyzed layer is 1.8 μm in langatate, 2.3 μm in langasite, and 2.9 μm in catangasite, which is much less than the powder particle size. The integral characteristics of the phase composition were thus examined under the actual experimental conditions. The accuracy of our 2θ angle measurements was 0.05° ; the method's sensitivity (the minimum amount of the measured phase) was ~ 1 wt %. The crystal lattice parameters at 25, 400, 600, and 700°C were determined according to the Bragg–Wulf relation using the reflexes from planes (4000) and (0002).

Temperature dependences of the crystal lattice parameters, based on theoretical data with allowance for thermal expansion and on our experimental data, were compared. The thermal expansion coefficient (TEC) in the range from room temperature to 1000°C and its anisotropy in catangasite and langatate crystals were determined in [8]. Based on these data, lattice parameters a_a and a_c were calculated using the formula for the hexagonal syngony in the investigated temperature range with allowance for thermal expansion along the X and Z axes:

$$\Delta_{HKL} = \frac{4H^2 + HK + K^2}{3} \frac{\alpha_a}{a_a^2} + \frac{L^2}{a_c^2} \alpha_c \Delta T, \quad (2)$$

where $\Delta_{HKL} = \frac{\Delta d_{HKL}}{d_{HKL}}$, ΔT is the change in temperature; d_{HKL} is the interplanar spacing; $\alpha_a = \alpha_{11}$ is the

thermal expansion of the crystal along the X axis; and $\alpha_c = \alpha_{33}$ is the thermal expansion along the Z axis.

RESULTS AND DISCUSSION

Positions of the reflexes on the diffraction patterns of langasite, langatate, and catangasite crystals obtained from powder samples at room temperature and during annealing with rising temperature in *vacuo* over 1.5 h correspond to the standard reflexes of the investigated crystals that are listed in the powder diffractometry database ICDD PDF-2 (2006). Analysis of the diffraction patterns allowed us to monitor the dynamics of changes in the phase composition and the elementary unit parameters of the investigated samples upon heating. It was found that with annealing, the phase composition of all investigated samples was stable up to 1000°C : the measured diffraction reflexes were in a good agreement with the standard values, and no reflexes corresponding to other phases were observed (Table 2).

We found no impurity phases or irregularities in any of our langasite, langatate, and catangasite crystals, in contrast to the results of [9] where an impurity phase of Ga₂O₃ was observed in langatate samples even at room temperature. The authors of [9] also observed a number of specific features, e.g., the broadening, asymmetry, and splitting of some reflexes at narrow angles (2θ from 12° to 36°).

Let us consider processes that occur in the investigated powders upon high-temperature treatment using the diffraction patterns of langatate as an example. Diffractograms of langatate obtained at room temperature and at 600°C are shown in Figs. 2a and 2b. The intensities of the different diffraction reflexes change

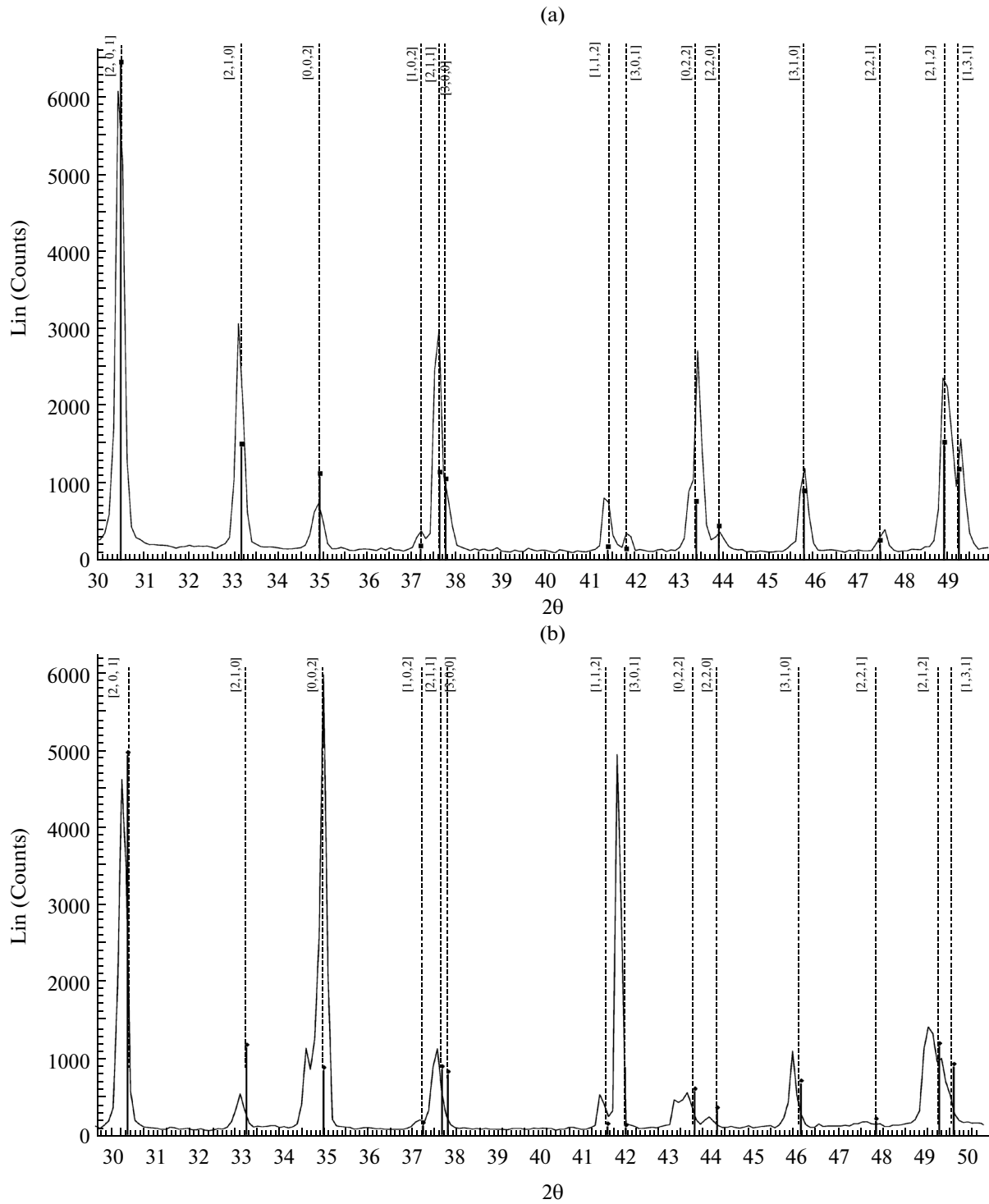


Fig. 2. Diffraction fragments of langatate powder at (a) 25°C and (b) 600°C.

as the temperature grows, due to the relaxation of mechanical strains that appear after the grinding of a single crystal, and primary recrystallization takes place: imperfect grains of the investigated phase are replaced with more perfect ones, and the intensities of

the reflexes corresponding to planes with faster grain growth increase.

The powder particles are crystallites with different sizes and random (mainly lamellar) shapes that determine the primary packing texture. As the temperature

grows, the recrystallization and thermal expansion of the crystallites alter the packing texture typical of imperfect polycrystals.

Finding a correct theoretical description of grain growth in polycrystalline materials is a rather complicated task that requires detailed knowledge of many structural and geometrical parameters of the grains, grain interfaces, and grain ensembles, and of the effect these parameters have on the mobility and energy of grain interfaces. Although there are now many theoretical approaches to describing grain growth in large-grained polycrystals, the laws governing these processes are still under intense study in light of the patterns that have been revealed experimentally.

Grain growth in polycrystals usually follows a standard scenario that involves the migration and merging of grain interfaces. These increase the average grain size and lower the number of grains in a polycrystal. Grain growth due to the migration and merging of grain interfaces is usually considered to be the only mechanism of grain growth in large-grained polycrystals.

The lower free energy of a grain interface, the total area of which shrinks as the grains grow, is the main force behind this process. It tends to reduce the grain interface density or, in other words, the volume fraction of the material that comprises the interface. In addition to this driving force, there are forces that impede growth. The main hindrance to grain growth in typical large-grained polycrystals is the limited mobility of the migrating grain interfaces. Competition between the driving and impeding forces of grain growth determines the stability of nanocrystalline and polycrystalline structures with respect to the increase in their average grain size.

Recrystallization is more prominent in the regions of diffraction patterns with two reflexes from planes (0002) and $(21\bar{3}0)$ (Fig. 3). The intensity rises by a factor of 6 along direction [0002] ($\parallel Z$) as the temperature grows, while along direction $[21\bar{3}0]$ ($\perp Z$) it falls by a factor of 6, due to the growth of the grains with surface Z being accompanied by the merging the grains with prismatic orientations.

The peak half-width on the catangasite diffraction pattern falls by 30%, while the annealing temperature reaches 900°C and then begins to rise again (Fig. 4) due to strain relief and the healing of defects that appear during the growth and subsequent treatment of crystals (especially in grounded samples) at temperatures of up to 1000°C. We find that grains with reflex $(11\bar{2}1)$ are absorbed at 900°C by larger grains with the same reflex $(11\bar{2}1)$.

Table 2 presents the phase composition of the investigated powders at different annealing temperatures in vacuo. No additional phases were observed upon annealing below 1000°C. Only at 1200°C do

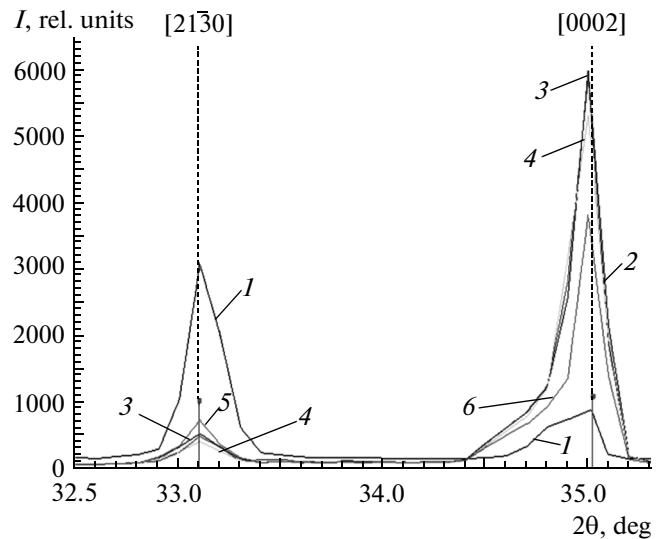


Fig. 3. Temperature behavior of the intensities of diffraction reflexes from planes (0002) and $(21\bar{3}0)$ in langatate crystals. (1) 25°C; (2) 400°C; (3) 600°C; (4) 800°C; (5) 1000°C; (6) 1100°C; standard diffraction reflexes of langatate.

additional diffraction reflexes appear in the diffractograms of all the investigated crystals, due to the partial decomposition of the main phase in the surface regions of the crystals upon high-temperature annealing. New diffraction reflexes that emerged at 1200°C can be seen in Fig. 6.

Analysis showed that additional phases of $\text{La}(\text{GaO}_3)$ and La_2O_3 are formed in langasite crystals at 1200°C; at the same temperature $\text{La}(\text{TaO}_4)$, $\text{La}(\text{GaO}_3)$, and TaO_2 appear in langatate crystals. Lanthanum and tantalum have high chemical reactivity, especially at high temperatures, and easily react with oxygen to produce oxides.

The effect of thermal annealing in vacuo on the composition of $\text{La}_3\text{Ga}_5\text{SiO}_{14}$ crystals (LGS) was investigated in [10] via X-ray photoelectron spectroscopy (XPS) and X-ray fluorescence analysis (XFA).

The first annealing experiment at 1050°C over 30 min showed that the crystal changed color and the chemical composition of the platelet surfaces (gallium concentration decreased sharply) was altered. The obvious change in composition was revealed by surface-sensitive XPS (Fig. 5). Parameter K/K_0 (where K is the ratio of the intensity of the photoelectron line of gallium to that of lanthanum, and K_0 is the initial value before annealing) grows as the depth of analysis increases. In other words, the gallium concentration grows with depth and reaches the one prior to annealing, but it does not attain this value even after etching for 60 min (i.e., at depths of 120–240 nm). The size of the region of altered composition was evidently greater than the etching depth.

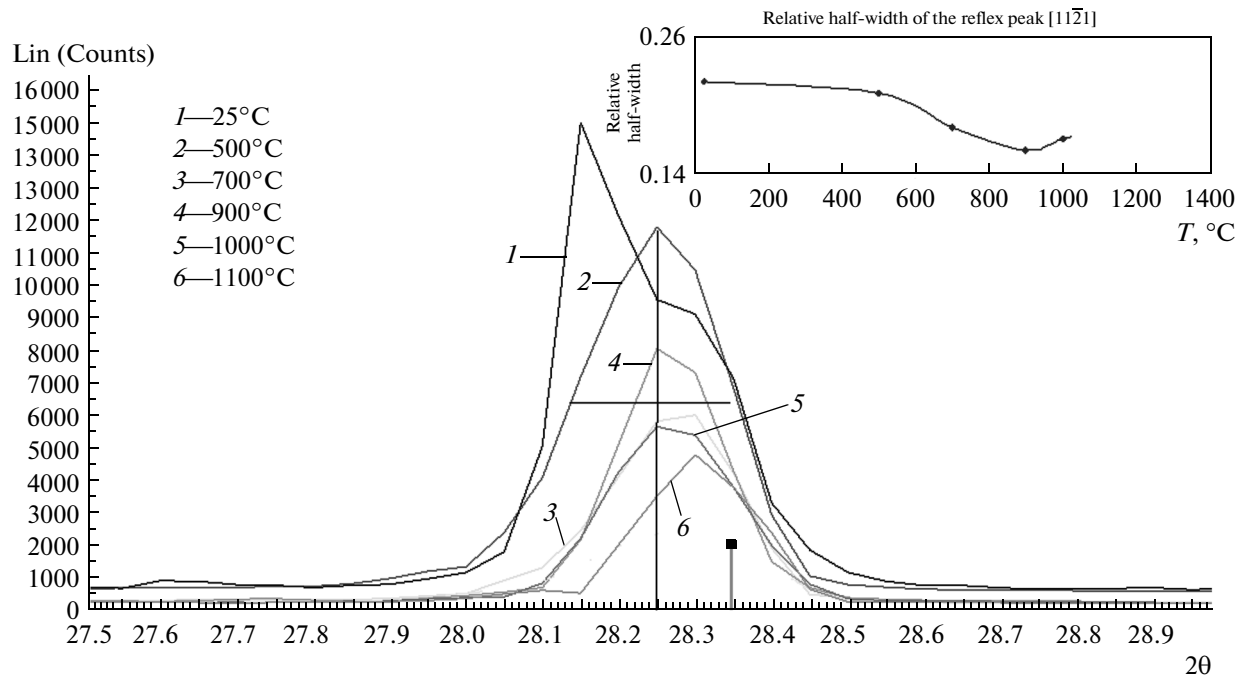


Fig. 4. Changes in the half-width of the reflex peak from plane (11 $\bar{2}$ 1) in catangasite crystals with rising annealing temperature in vacuo. ■ Standard diffraction reflexes of catangasite.

XFA revealed a change in the crystals' composition, though it was not as obvious [9]. The value of K_{vol} (the ratio of the average GaK/LaL line intensities after annealing, divided by the initial ratio) was 0.98 ± 0.02 . This means that up to 2 at % gallium was lost in the 10–60- μ m-thick surface layer.

The authors of [9] proposed the following chain of events that lead to such prominent changes in the

chemical composition of the surface of LGS platelets upon heating in vacuo: oxygen desorption \rightarrow the number of oxygen vacancies increases \rightarrow gallium's active valence falls to 1 \rightarrow clusters of volatile Ga_2O form \rightarrow Ga_2O evaporates from the surface.

The diffraction pattern of langatate powder obtained after prolonged (up to 6 h) annealing in air at 1200°C is shown in Fig. 6. The formation of volatile Ga_2O in the langatate crystal upon heating in air is hampered by the high partial pressure of oxygen, and no additional phases are seen in the diffraction pattern up to a temperature of 1200°C, in contrast to annealing in vacuo which results in additional phases above 1000°C, testifying to the higher thermal stability of langatate crystals in air.

No phase transitions were revealed in diffraction patterns recorded in steps of 200°C upon heating in the range below 700°C. The interference maxima were shifted due to the thermal expansion of the crystal, allowing us to calculate the lattice parameter in the temperature range of 25 to 700°C.

Calculated lattice parameters a_a and a_c , allowing for thermal expansion and experimental values for reflexes from the planes (0002) and (4000) in the range from room temperature to 800°C, are presented in Table 3. It turns out that parameter a_a of catangasite in the close packing plane, measured experimentally by means of high-temperature phase analysis, grows with temperature according to TEC, while the value of a_c ,

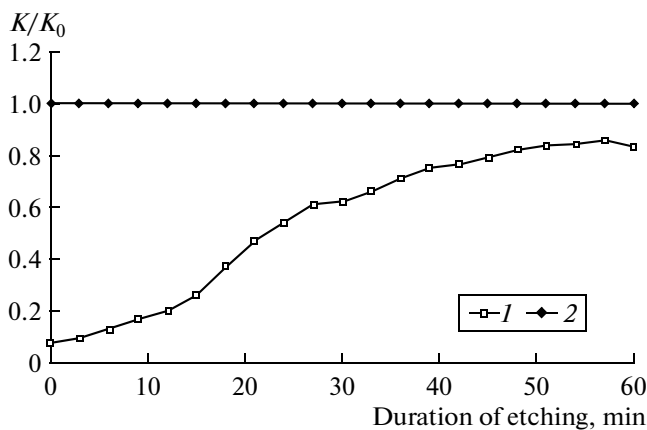


Fig. 5. Dependence of parameter K/K_0 on duration of etching by Ar^+ ions for the Z cross section in langasite crystals: (1) after annealing at 1000°C for 5 h; (2) K_0/K_0 (sample before annealing) [10].

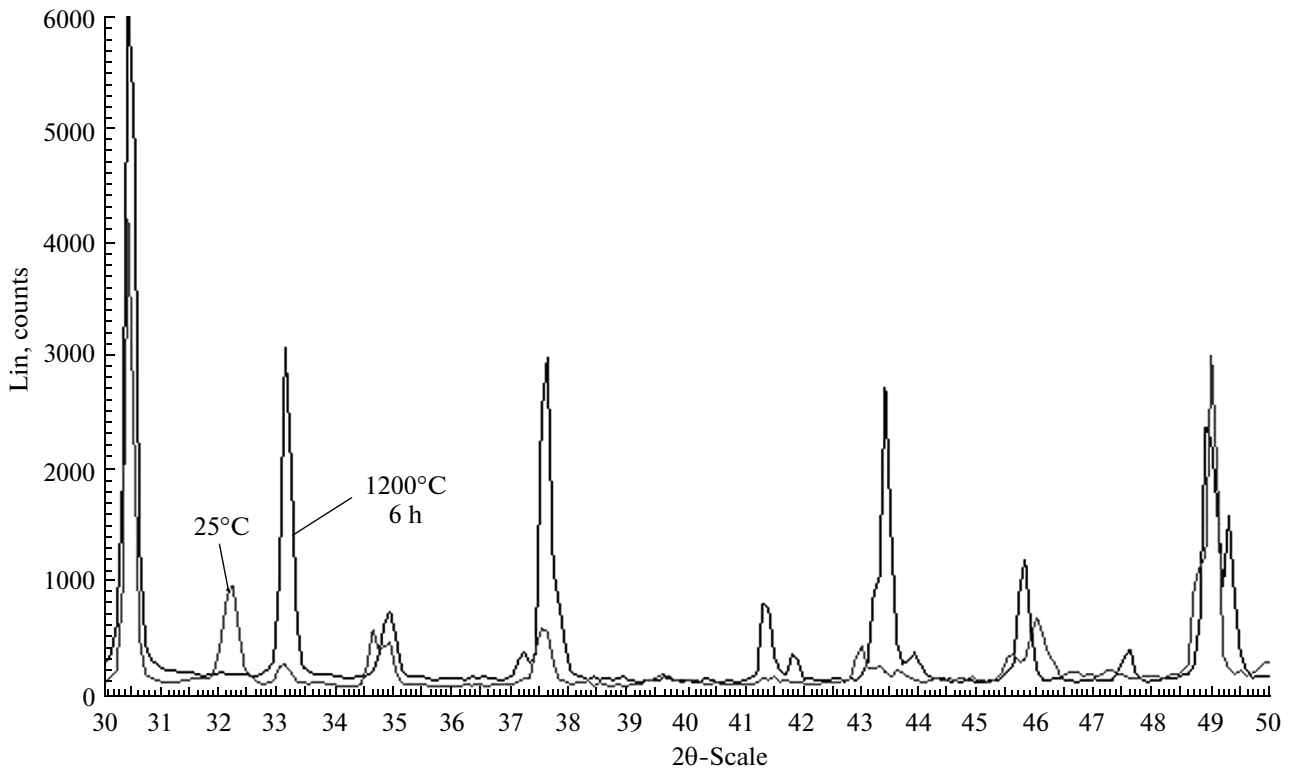


Fig. 6. Fragment of langatate diffraction pattern after annealing in air for 6 h at 1200°C.

which corresponds to the direction across the polyhedra layers, has a weak temperature dependence. This phenomenon can be analyzed using the data presented in [10], where different ways of including Ga in the lattice of langasite crystals $\text{La}_3\text{Ga}_5\text{SiO}_{14}$ and $\text{La}_3\text{Ga}_{5.14}\text{Si}_{0.86}\text{O}_{14}$ at room temperature were considered. A gallium ion can occupy three positions in the crystal lattice: octahedral, tetrahedral, and trigonal-pyramidal one, the latter can also be occupied by a Si ion (Fig. 1). The author showed that the lattice parameters increase as

the Ga content grows, which is in agreement with the ion radii of Ga and Si ($r_{\text{Ga}} > r_{\text{Si}}$). Gallium ions, due to their high diffusion mobility, move to the interstitial positions upon heating to 1000°C and are replaced in the polyhedra either by vacancies or by silicon ions which have shorter radii. Substituting silicon ions for gallium ions reduced the lattice parameter, thereby compensating for the thermal expansion of the crystal. No decomposition of the main phase below 1000°C was observed using X-ray diffractometry.

Table 3. Catangasite crystal lattice parameters from room temperature to 700°C, calculated on the basis of reflexes (4000) and (0002) from planes *X* and *Z* allowing for TEC, and experimental values

Temperature, °C/Lattice parameter	25	400	600	700
Reflex (0002)				
<i>c</i> experimental	5.1932	5.196	5.196	5.196
<i>c</i> calculated	5.1932	5.209	5.2183	5.2232
TEC, 10 ⁻⁶ K ⁻¹	2.3	8.26	8.51	8.64
Reflex (4000)				
<i>a</i> calculated	8.0982	8.1197	8.1338	8.1411
<i>a</i> experimental	8.0982	8.1276	8.1272	8.1302
TEC, 10 ⁻⁶ K ⁻¹	0.36	5.4	5.8	5.94

CONCLUSIONS

The phase composition of langasite family crystals ($\text{La}_3\text{Ga}_5\text{SiO}_{14}$, $\text{La}_3\text{Ta}_{0.5}\text{Ga}_{5.5}\text{O}_{14}$, and $\text{Ca}_3\text{TaGa}_3\text{Si}_2\text{O}_{14}$) was found to be stable upon annealing in vacuo at temperatures below 1000°C and in air below 1200°C .

High-temperature X-ray diffractometry revealed the partial decomposition of the initial phase upon heating above 1000°C in vacuo, accompanied by the formation of gallium-depleted oxides of the main elements due to the production of volatile gallium protoxide and loss of gallium in the surface layer of the crystals. Annealing in vacuo at 1200°C led to the emergence of new reflexes (in addition to peaks of the main phase) that belonged to secondary and tertiary gallium-depleted phases within the studied crystals (La_2O_3 , $\text{La}(\text{GaO}_3)$, TaO_2 , $\text{La}(\text{TaO}_4)$, and so on).

The heating of the powders was accompanied by recrystallization with dominant grain orientation Z and by a lower number of defects and mechanical strains.

Annealing in vacuo at 1000°C changes crystal lattice parameter a_a according to the thermal expansion coefficient. The high diffusion mobility of gallium ions shifts ions into interstitial positions and lowers the lattice parameter, thus compensating for the thermal expansion in plane (0001), the most stable close-packed plane in a langasite crystal.

REFERENCES

1. Mill, B.V. and Pisarevsky, Yu.V., *Proc. 2000 IEEE Int. Frequency Control Symp.*, Kansas City, 2000, pp. 133–144.
2. Mill', B.V., Butashin, A.V., Khodzhabagyan, G.G., et al., *Dokl. Akad. Nauk SSSR*, 1982, vol. 264, no. 6, pp. 1385–1389.
3. Buzanov, O.A., RF Patent 2108418, C1, IPC6 C 30 B 29/34, 15/00, *Byull. Izobret.*, 1998, no. 10, p. 3.
4. Koznov, G.G., RF Patent 2126063, C1, IPC6 C 30 B 29/34, 15/00, *Byull. Izobret.*, 1998, no. 4, p. 3.
5. Medvedev, A.V., The way for researching and developing technologies and structures for new piezoelectrical devices based on lanthanum-gallium silicate monocrytals, *Cand. Sci. Eng. Dissertation*, Moscow, 2009.
6. Andreev, I.A., *Zh. Tekhn. Fiz.*, 2006, vol. 76, no. 6, pp. 80–86.
7. Zengmei, W. and Duorong, Y., *J. Crystal Growth*, 2003, vol. 275, pp. 398–403.
8. Kugaenko, O.M., Uvarova, S.S., Krylov, S.A., et al., *Bull. Russ. Acad. Sci. Phys.*, 2012, vol. 76, p. 1406.
9. Tyunina, E.A., Kuzmicheva, G.M., et al., *Vestn. Mosk. Inst. Tonk. Khim. Tekhnol.*, 2010, vol. 5, no. 1, pp. 57–68.
10. Malinkovich, M.D., Skryleva, E.A., and Shul'ga, N.Yu., in *Tezisy dokladov Chetyrnadtsatoi Natsional'noi konferentsii po rostu kristallov i IV Mezhdunarodnoi konf. "Kristalofizika XXI veka"* (Proc. 14th National and 4th Int. Conf. on Crystals Growth "Crystal Physics of 21st Century"), Moscow, 2010, vol. 1, p. 395.

Translated by S. Efimov